HIGH-IMPEDANCE SURFACES BASED ON SELF-RESONANT GRIDS. ANALYTICAL MODELLING AND NUMERICAL SIMULATIONS

C. R. Simovski

Department of Physics
St. Petersburg Institute of Fine Mechanics and Optics
197101, Sablinskaya 14, St. Petersburg, Russia

A. A. Sochava

Department of Radiophysics
St. Petersburg State Polytechnical University
195251, Polytekhnicheskaya 29, St. Petersburg, Russia

Abstract—A new variant of artificial high-impedance surfaces is suggested and studied. This is a thin composite layer consisting of a dielectric layer with a planar self-resonant grid from metal strips on its surface. Every grid element is connected to the ground plane with a metal pin. We use an analytical model which has been recently developed for a similar structure. The advantages of the new structure (decreasing the resonant frequency for fixed period and thickness, further angular stabilization of surface impedance for the TE-incidence of waves) are studied and explained. The analytical model is compared with numerical simulations. It predicts quite well the resonant frequencies of the artificial surface for different angles of incidence however is not enough accurate for calculating the values of the surface impedance.

5 Conclusion

References

1. INTRODUCTION

In modern microwave techniques printed circuit antennas are widely used. As a rule, these antennas are positioned on a surface of a dielectric layer with a metal ground plane on the opposite side of the slab. In practice, the thickness h of the metal-backed dielectric layer must be very small compared to the wavelength λ in free space. When $h < \lambda_d/4$, where $\lambda_d = \lambda/\sqrt{\varepsilon}$ is the wavelength in the dielectric medium, the electromagnetic interaction of the antenna current with the ground plane is destructive and leads to practically significant decreasing of the antenna radiation resistance. When the dielectric permittivity is very high and $h \approx \lambda_d/4$, the influence of the ground plane becomes constructive. However, the zenithal radiation is still very small in this case as compared with the same antenna in free space. It is so because 60–70 percent of the antenna radiation is spent for the excitation of lateral waves in the dielectric layer [1]. In 1998–1999 it was proposed to replace usual dielectric layers by high-impedance surfaces (HIS) (e.g., [2]). A HIS operates as a magnetic wall when the working frequency of the antenna lies within the HIS resonant band. In this way one can dramatically improve the antenna efficiency (e.g., [2, 3], and [4]). However, it is not very easy to design an impenetrable HIS satisfying practical requirements. To be practically suitable, the substrate thickness must be small compared to λ and the resonant bandwidth must not be very narrow to allow radiation of broadband signals. Actually, it is very desirable to obtain the regime of a magnetic wall for the whole spatial spectrum of the antenna radiation. In fact, the HIS:S developed in cited works do not exhibit a uniform surface impedance with respect to different spatial harmonics. The uniform Z_s depending on the frequency and independent on the incidence angle θ would allow us to apply the impedance boundary conditions for the whole radiation of an antenna positioned in the proximity of a HIS (perhaps, separated from it with a very thin dielectric layer). However, Z_s calculated and measured in the cited works is a *plane-wave* surface impedance which dramatically depends on the incidence angle θ. The functions $Z_s^{TE}(\omega)$ and $Z_s^{TM}(\omega)$ corresponding to the two polarizations of the incident wave (TE and TM, respectively) are different. In the works [2] and [4] a very approximate analytical theory of the plane-wave surface impedance has been developed for the case of the wave normal incidence to the mushroom structure. The mushroom structure is a

dense array of square or hexagonal patches on a surface of a dielectric layer. Every patch is connected to the ground with a vertical metal pin. The theory [4] was generalized to the case of oblique TE incidence in our work [5]. In another work [6] we noticed that the presence of vias (originally introduced in order to suppress the lateral TM waves inside the mushroom structure [4]) helps to obtain a stable resonant frequency for different θ for the case of the TM incidence. This is the case, when the electric field vector of the incident wave contains a component directed along the vias which excites the vertical current in them. A possible explanation of this stabilization effect was given in [6]: the array of grounded metal pins operates as a layer of the so-called *wire medium*. Recently, we have shown in [7] that TM-polarized incident waves excite two eigenwaves in wire media. One is an extraordinary mode that has a stop-band at low frequencies. The other is then the TEM mode. Since the period of the patch array is very small compared to λ_d, the extraordinary wave decays very rapidly along the vias, and we can assume that its influence is negligible. The only important solution is the TEM wave. Its propagation factor has two components: the normal to the interface component is equal to the wave number of the dielectric host medium $k_d = \omega\sqrt{\varepsilon\varepsilon_0\mu\mu_0}$, and the tangential component equals that of the incident wave. The energy propagates strictly along the vias with the propagation factor k_d and, therefore, the surface impedance of the mushroom structure turns out to be independent on the incidence angle θ [6]. However, this is a very approximate result since in our speculations we ignore the influence of the evanescent mode. The measurements in [6] show that the resonant frequency of Z_s for the TM case of the wave incidence weakly depends on θ (unlike the TE case when the vias are not excited and the resonance of a mushroom structure dramatically shifts versus the incidence angle). However, the shape of the curve $Z_s(\omega)$ is still different for different θ. One of the ideas suggested in [6] was to obtain a really stable (with respect to θ) frequency dependence of Z_s for the TM case. Only this allows us to consider the surface impedance $Z_s^{TM}(\omega)$ as a uniform parameter of the artificial surface for a broad spectrum of TM spatial harmonics radiated by an antenna.

With this purpose we suggested in [6] a self-resonant grid instead a grid of patches. Our expectations were the following: in the mushroom structure [2] the grid of patches behaves as a screen which reduces the influence of the array of vias. The self-resonant grid is made from thin metal strips, and a large part of its surface is penetrable for incident waves. Therefore, the array of vias is illuminated better by the incident wave, which stabilizes the function $Z_s^{TM}(\omega)$ with respect to the parameter θ more efficiently than in the case of a mushroom

structure. So, in [6] we proposed to use planar spirals instead of square patches. The experimental data confirmed that the structure behaves as expected.

In the present paper we develop this new type of HIS. Instead of a grid of patches, we propose a structure with a series-resonant grid instead of a grid of patches which possesses two advantages with respect to the mushroom structure: lower resonant frequency and better angular stability for the TE-polarized incident waves.As well as the structure suggested in our previous work [6], our new HIS (from elements shown in Fig. 2) has $Z_s^{TM}(\omega)$ weakly depending on θ. Additionally, the resonant frequency is lower than that of the mushroom structure and than that of the structure suggested in [6]. This is an important advantage, since this property allows to decrease the dimensions of the structure for a fixed resonant frequency. Also, our new structure shows a certain stabilization of $Z_s^{TE}(\omega)$ with respect to variations of θ (unlike the structure from [6]). The surface impedance of the structure from [6] is also more stable (versus θ) for the TE-incidence than that of the mushroom structure, however the structure introduced in the present paper show further angular stabilization. The three structures under comparison (top view) are shown in Fig. 3.

2. ANALYTICAL MODEL

2.1. General Formulae

Consider a planar array of conducting elements located on the surface ($z = 0$) of a dielectric shield of thickness h. Let the structure be illuminated by a plane wave. If the grid period D is small compared to λ_d the tangential component of the electric field in the grid plane averaged over the grid periods is simply proportional to the averaged current induced in the grid [8]. The averaged current $< J >$ is equal to the jump of the tangential component of the averaged magnetic field across the grid plane. Then we have

$$\langle E_t \rangle (z = +0) = Z_g \langle J \rangle \equiv Z_g \left(\langle H_t \rangle (z = +0) \ - \langle H_t \rangle (z = -0) \right). \quad (1)$$

In (1) we assumed that the grid is practically isotropic in the horizontal plane ($x - y$), i.e. there is no polarization transformation of the averaged field with respect to the incident wave field. Then the grid impedance Z_g determined by (1) is a scalar value [8]. The surface impedance is determined by the relation

$$\langle E_t \rangle (z = +0) = Z_s \langle H_t \rangle (z = +0), \quad (2)$$

and in terms of the transmission-line approach it can be expressed as a parallel connection of Z_g and the surface impedance of the dielectric shield Z_d:

$$Z_s = \frac{Z_g Z_d}{Z_g + Z_d}. \tag{3}$$

This transmission-line approach was successfully validated in our study [5] for the case of a patch array on the shield surface. It was shown that the error related with the approximate formula (3) is very small for practically important cases. The resonance at which the structure behaves as a magnetic wall corresponds to the case $X_g(\omega) + X_d(\omega) = 0$, where $X_s = \text{Im}(Z_s)$, $X_d = \text{Im}(Z_d)$. Let us denote the solution of this equation as $\omega = \omega_0$. The dielectric shield (with or without vias) can be considered as a shortened transmission line, and the surface impedance $Z_d = R_d + jX_d$ of a thin metal backed substrate ($h < \lambda_d(\omega_0)/4$) is inductive. Therefore, we need to have a capacitive grid to form a HIS: $Z_g = R_g - j|X_g|$.

Let the substrate be periodically perforated by metal pins. In the case of the TE-incidence Z_d is not affected by the pins and we have [5]:

$$Z_d^{TE} = \frac{j\eta}{\sqrt{\varepsilon - \sin^2 \theta}} \tan k_{zd} h, \tag{4}$$

where $\eta = \sqrt{\mu_0/\varepsilon_0}$ is the wave impedance of free space and $k_{zd} = \omega \sqrt{\varepsilon - \sin^2 \theta} \sqrt{\varepsilon_0 \mu_0}$ is the vertical component of the wave vector of the refracted wave. For the TM-case Z_d can be considered as the surface impedance of a thin layer of the wire medium. As we have already noticed, at low frequencies the wire medium is practically a TEM transmission line with the energy propagating strictly along z. The surface impedance of this shortened line does not depend on the incidence angle, and we obtain:

$$Z_d^{TM} = \frac{j\eta}{\sqrt{\varepsilon}} \tan k_d h, \tag{5}$$

where $k_d = \omega \sqrt{\varepsilon \varepsilon_0 \mu_0}$.

The grid of perfectly conducting patches separated with thin slits of width w from one another is positioned on the dielectric interface. Denote its grid impedance as $Z_g = Z_p$. For Z_p two explicit expressions were obtained in [5]:

$$Z_p^{TE} = \frac{\eta}{2j\alpha \cos^2 \theta} \tag{6}$$

for TE-incidence, and

$$Z_p^{TM} = \frac{\eta}{2j\alpha} \tag{7}$$

for TM-incidence. Here we denote

$$\alpha = \frac{k'D}{\pi}\left[\log\left(\frac{2D}{\pi w}\right) + \frac{\zeta(3)}{2}\left(\frac{k'D}{2\pi}\right)^2 + \frac{3\zeta(5)}{2^3}\left(\frac{k'D}{2\pi}\right)^4 + \ldots\right],$$

where ζ is the Riemann zeta-function and $k' = \omega\sqrt{\varepsilon_0\mu_0}\sqrt{(\varepsilon+1)/2}$. If $|k'D| \ll 2\pi$, the terms with ζ are negligible, the parameter α is proportional to the frequency, and both relations (6) and (7) can be represented in the form

$$Z_p = r_g + \frac{1}{j\omega C_g}. \tag{8}$$

In (8) the effective grid capacitance C_g depends on the angle of incidence for the TE case and does not depend on that for the TM case. If the dielectric losses are negligible ($\text{Im}(\varepsilon) \approx 0$), the loss term r_g in (8) vanishes.

A self-resonant grid (see e.g., [9]) whose unit cell contains both effective capacitance C_g and inductance L_g has the grid impedance (at low frequencies in the case when the dielectric losses are negligible) which can be presented in the form

$$Z_g = \frac{1}{\cos^2\theta}\left(j\omega L_g + \frac{1}{j\omega C_g}\right) \tag{9}$$

for the TE-case and in the form

$$Z_g = \left(j\omega L_g + \frac{1}{j\omega C_g}\right) \tag{10}$$

for the TM-case. In both (9) and (10) it is assumed that L_g and C_g do not depend on the incidence angle.

In the work [6] a grid of spiral-shaped metal elements was proposed to substitute the patch array with the purpose to make the function $Z_s^{TM}(\omega)$ be more stable with respect to the variations of the incidence angle θ. This grid is shown in Fig. 1. The resonant frequency of the structure containing a grid of spiral-shaped metal elements is rather close to that of the mushroom structure. In our comparisons we assumed that the main parameters of the two structure are same: the period of the patch array and that of the array of spirals, the width of the slit between two adjacent patches and that between two adjacent spirals, the dielectric thickness h, the permittivity ε and the pin radius ρ. From the comparison of (8) and (10) one can see that the equivalence
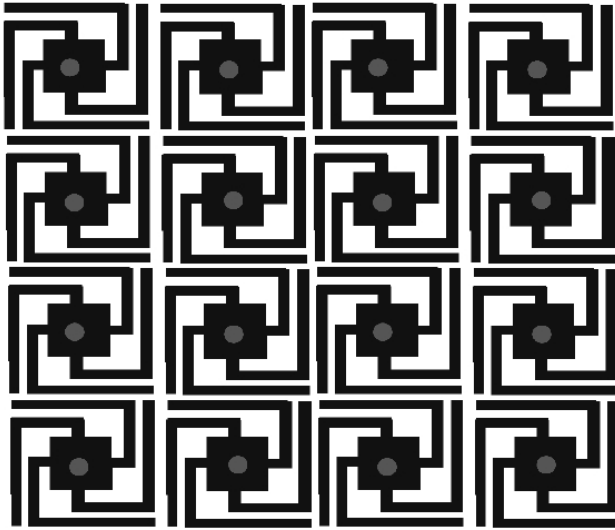
Figure 1. A grid of spiral-shaped elements from [6]. Top view. Circles at the patch centers show the connections of the vias.

of the resonant frequencies of the two HIS means the equivalence of the grid impedances of the two structures:

$$\frac{1}{j\omega C_g^p} = \frac{1}{j\omega C_g^{sp}} + j\omega L_g^{sp}, \tag{11}$$

where the upper indices p and sp refer to the patches and spirals, respectively. In fact, the spiral element has a smaller area than the patch, and, therefore, $C_g^{sp} < C_g^p$, however the deficiency of the capacitance is compensated by the presence of inductance L_g^{sp}. However, this compensation is only partial, and the resonant frequency of the structure with a spiral array [6] turns out to be a bit higher than that of the mushroom structure (patch array).

In the present work we suggest another variant of the spiral-shaped element. Here our purpose is not only to stabilize $Z_s^{TM}(\omega)$ with respect to the variations of θ but also to decrease the resonant frequency ω_0 for fixed geometrical parameters of the structure.

Of course, a HIS whose resonant frequency is lower than that of a mushroom structure is known. This is a structure with two patch arrays located at two different levels and sandwiched with a thin dielectric film [10]. However, the structure we suggest is simpler and cheaper in fabrication, because there is only one dielectric layer

in the structure, and only one planar grid on its surface. Notice, that the multilevel mushroom structure from [10] possesses a very narrow band due to its comparatively high effective grid capacitance and small inductance. For the case of TE-incidence the resonant frequency of mushroom structures is unstable with respect to θ, and it shifts significantly to higher frequencies when θ grows. This shift is smaller for the structure from [6], however our modification is once more stable in this meaning.

The geometry of the new spiral element and the dimensions for which we have made analytical calculations and numerical simulations are shown in Fig. 2.
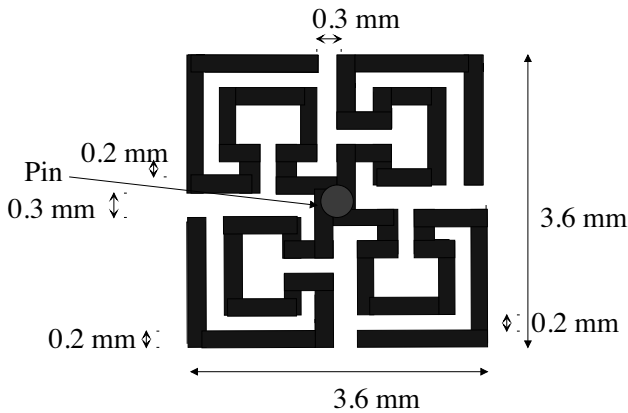

Figure 2. A spiral-shape element with loops. Geometrical parameters. Circle in the center shows the connection of the via.

We compare the structure in which the grid of such elements is positioned on the interface of the dielectric shield (the center of every element is connected to the ground plane with a via) with two basic HIS. The first one is the structure with spiral elements suggested in [6]. The second one is the mushroom structure. In Fig. 3 we show both these grids in comparison with the grid we suggest in the present paper. The comparison of the three structures implies, of course, that the main parameters are the same: the shield thickness $h = 6.1\,\mathrm{mm}$, the permittivity $\varepsilon = 2.17 - j0.02$, the grid element size $d = 3.6\,\mathrm{mm}$, the grid period $D = 3.9\,\mathrm{mm}$, the radius of vias $\rho = 0.3\,\mathrm{mm}$.

2.2. Calculation of L and C Parameters

Calculating L_g and C_g for the grid of spiral-shaped elements we neglect the imaginary part of ε, since there is no adequate model which could

Figure 3. The three objects of comparison (top view): a grid of spiral-shaped elements with loops (left), a grid of patches (center), and a grid of spiral-shaped elements without loops (right).

describe the influence of dielectric losses within the frame of the circuit model of the grid unit cell. However, when we calculate Z_d we take into account the dielectric losses, and in this way we avoid infinite values of Z_s and obtain a non-zero real part of the surface impedance.

Consider the inductance of the spiral element which is equal to L_g, assuming that the grid is illuminated by a normally incident wave. Notice that for any polarization of the electric field four identical portions of the spiral are excited identically, and the inductance of the spiral element is equal to $L_g = 4L_1$, where L_1 is the inductance of a one-quarter part of the whole element. We decompose this part of the spiral element into 11 straight pieces as it is shown in Fig. 4. The total inductance of the structure from pieces 1...11 is the sum of the self-inductances of the straight strips and their mutual inductances:

$$L_1 = \sum_{i=1}^{11} L_i + \sum_{i \neq j}^{11} M_{ij}. \tag{12}$$

Self-inductances for straight pieces $i = 1 \dots 11$ can be calculated as follows [11]:

$$L_i = \frac{\mu_0 l_i}{2\pi} \left[\log \frac{2l_i}{w} + \frac{1}{2} \right], \tag{13}$$

where w is the strip width and l_i is the piece length. Since the splits between pieces 1 and 9 and 3 and 7 are rather small, we can consider the system of two strips 3+7 (and the system of two strips 1+9) as a whole straight strip with length $l_3 + l_7$ (and $l_1 + l_9$, respectively). The mutual inductance of two orthogonal strips is negligible compared to the mutual inductances of two parallel strips. The mutual inductances of two parallel strips M_{ij} were calculated with the formula (2-83) from
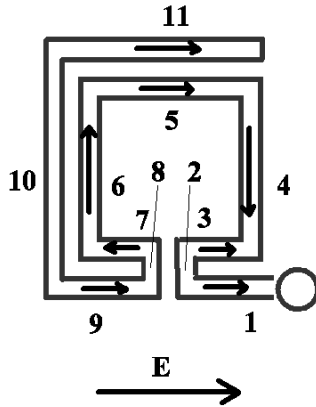
Figure 4. Splitting one quarter of the spiral element into straight portions. Arrows show the direction of the current induced by a horizontal electric field.

[11]. This cumbersome formula can be simplified for the case when the strip width w is small compared to the distance between the centers of the strips:

$$M_{ij} = \pm\frac{\mu_0 a}{2\pi}\left[\log\frac{2(1+\sqrt{1+\xi^2})}{1+\sqrt{1+4\xi^2}} - \sqrt{1+\xi^2} + \sqrt{1+4\xi^2}\right]. \quad (14)$$

The following notations have been introduced: $\xi = L_{ij}/2a$, $a = (l_i + l_j)/2$ is the averaged length of two parallel pieces, and L_{ij} is the distance between their centers. The plus sign corresponds to the case when the directions of the induced current in $i-$th and $j-$th pieces are the opposite (and vice versa). Consider the case when the electric field is directed horizontally as it is shown in Fig. 4. Then there is no current in portion 10, and this strip does not contribute into L_1. The inductance L_1 is equal approximately to $0.6L_{\text{loop}}$, where L_{loop} is the inductance of the loop formed by pieces $3, 4, 5, 6$, and 7.

Capacitance C_{sp} between two adjacent spiral-shaped elements can be calculated starting with Sievenpiper's formula for the capacitance between two adjacent patches C_p [2]. We consider the spiral-shaped element V as a hollow patch whose filling ratio is smaller than 1. The filling ratio f is defined as the area of the metal surface of a spiral-shaped element with sizes $d \times d$ divided by the area of a square patch d^2. Then we obtain:

$$C_{sp} = fC_p = f\frac{d(\varepsilon + 1)\varepsilon_0 d}{\pi}\text{acosh}\frac{D}{D - d}. \quad (15)$$
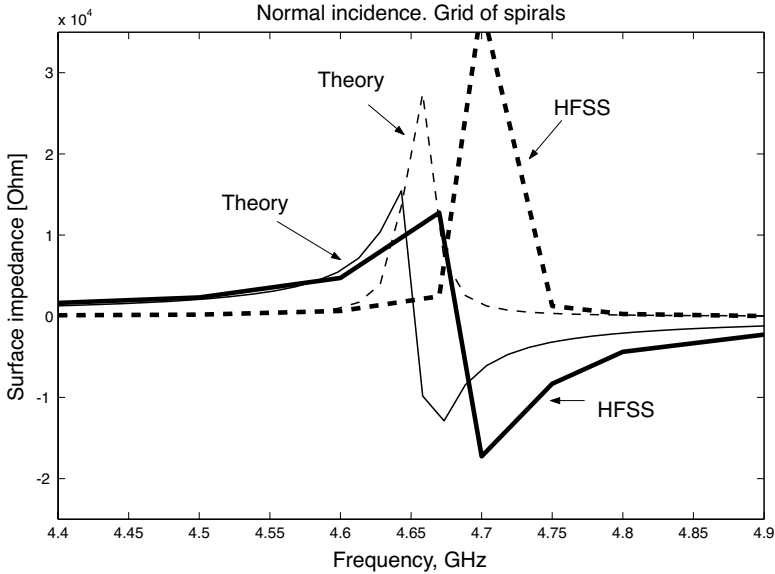
Figure 5. The surface reactance (solid) and resistance (dashed) of the structure containing a grid of spiral-shaped elements with loops. The normal incidence of the incident wave. Theory (thin lines) and simulations (thick lines).

The result for L_g and C_g is to be substituted into (9) and (10) in order to calculate Z_g. Then, we substitute Z_g together with formulae (4) and (5) into (3) and obtain the result for Z_s.

3. VALIDATION OF THE THEORY

In order to validate this approximate model we have made simulations using the well-known HFSS code, version 8. To calculate Z_s with the HFSS code we applied two different approaches. First, we calculated the amplitude of the reflected wave and expressed Z_s through the reflection coefficient R:

$$Z_s^{TE} = \eta \cos \theta \frac{R^{TE} + 1}{R^{TE} - 1}, \quad Z_s^{TM} = \frac{\eta}{\cos \theta} \frac{R^{TM} + 1}{R^{TM} - 1}. \tag{16}$$

Second, we calculated the tangential components of the fields E and H at the surface of the structure, made averaging, and found Z_s as the ratio $\langle E_t \rangle / \langle H_t \rangle$. Both approaches give practically the same result, which allows to conclude that our numerical results are reliable.
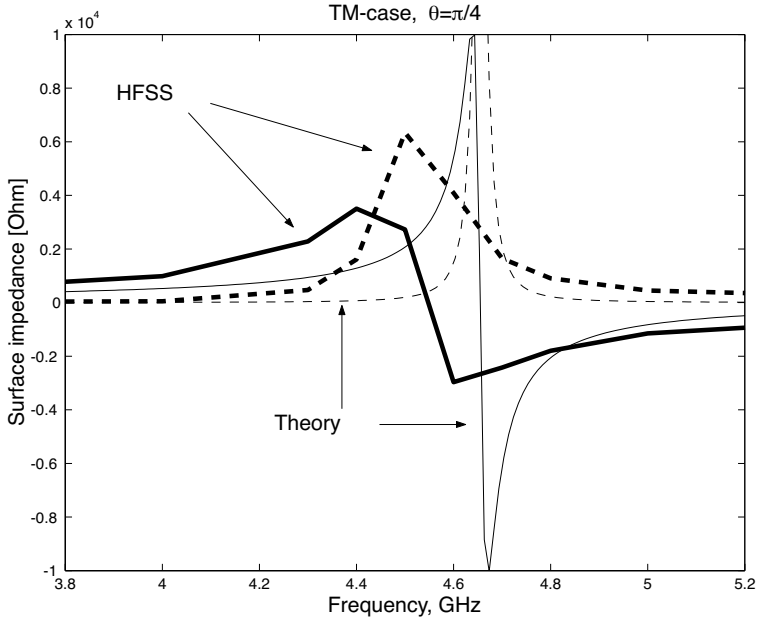
Figure 6. The surface reactance (solid) and resistance (dashed) of the structure containing a grid of spiral-shaped elements with loops. TM-incidence of the incident wave. Theory (thin lines) and simulations (thick lines).

In Fig. 5 we present the results of the comparison between the theory and simulations for a structure containing a grid of spiral-shaped elements with loops on the interface of a metal-backed dielectric layer with metal pins. Normal incidence of the exciting wave is assumed. The parameters of the structure are given above. We can conclude that our analytical model works reliably for this case. According to our theory, the resonant frequency for Z_s is equal to 4.64 GHz, whereas the simulations give the result 4.67 GHz.

In Figs. 6 and 7 we present a comparison between the theory and numerical simulations for the TM-case and the TE-case. Both these cases. correspond to $\theta = \pi/4$. The analytical model still gives a rather small error for the resonant frequency and for the resonant band, but the values of the surface reactance X_s and resistance R_s are described improperly. It is not surprising, becuase our model is quasi-static in what concerns the response of the spiral-shaped element. As any other circuit model, it does not take into account the electromagnetic interaction of the grid elements. The capacitive coupling between the
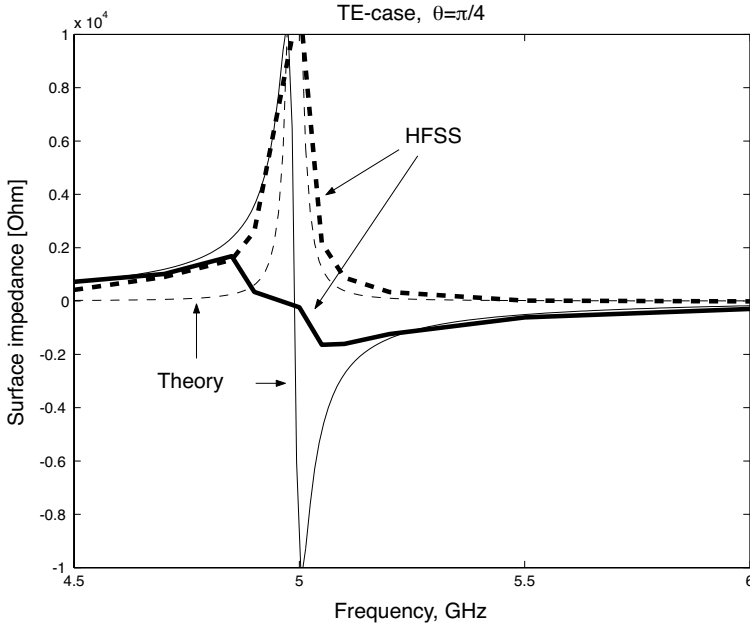
Figure 7. The surface reactance (solid) and resistance (dashed) of the structure containing a grid of spiral-shaped elements with loops. TE-incidence of the incident wave. Theory (thin lines) and simulations (thick lines).

adjacent elements of the grid is taken into account, but the far-zone interaction of the spiral-shaped elements is ignored. This is the main shortcoming of our theory.

4. COMPARISON WITH OTHER STRUCTURES

To study the advantages of the new structure we compared the numerical simulations of Z_s for this new design with those for two other objects (see Fig. 3). In Fig. 8 we present the comparison of the surface impedance for two structures. The first structure (thick lines) contains spiral-shaped elements with loops. The second structure (thin lines) contains metal patches (see Fig. 3, on the bottom). The resonant frequencies are 4.67 GHz (the first structure) and 4.93 GHz (the second one). Our new structure allows to decrease the resonant frequency by 7 percents.

In Fig. 9 we present a similar comparison for the case of TM- and TE-incidence, $\theta = \pi/4$. Comparing Fig. 9 with Fig. 8 we can conclude
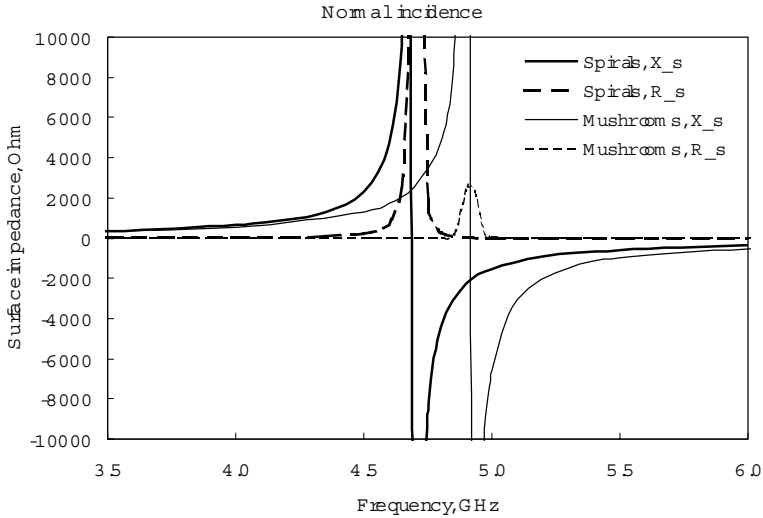
Figure 8. The surface impedance of two structures under comparison (HFSS simulations). Normal incidence. Thick lines: the structure containing a grid of spiral-shaped elements with loops. Thin lines: the mushroom structure.

that the frequency dependence of our structure is much more stable with respect to variations of θ than that of the mushroom structure. In Fig. 10 we compare our structure with its analogue from [6] (see Fig. 3, on the top). The resonant frequencies are 4.67 (first structure) and 5.18 GHz (second one). So, the suggested modification of the structure from [6] allows us to decrease the resonant frequency by 9 percents. This is a result of a rather high grid inductance L_g due to the presence of loops. The structure we suggest in the present paper possesses a lower resonant frequency with respect to both mushroom structure and structure with spiral elements which do not contain loops. Its surface impedance demonstrates the same stability with respect to the incidence angle as the structure from [6], and it is more stable for the TM-incidence than for the mushroom structure. An unexpected result was obtained for the TM-incidence. Comparing Fig. 7, TE-incidence with Fig. 8, we can see that the resonant frequency of our new structure shifts from 4.67 to 4.90 GHz when the angle θ varies from 0 to $\pi/4$, whereas the resonant frequency of the mushroom structure shifts from 4.93 to 5.46 GHz. For the structure from spiral-shaped elements without loops which was suggested in [6] the resonant frequency shifts from 5.2 to 5.6 GHz for the TE-case when θ is growing from 0 to $\pi/4$.
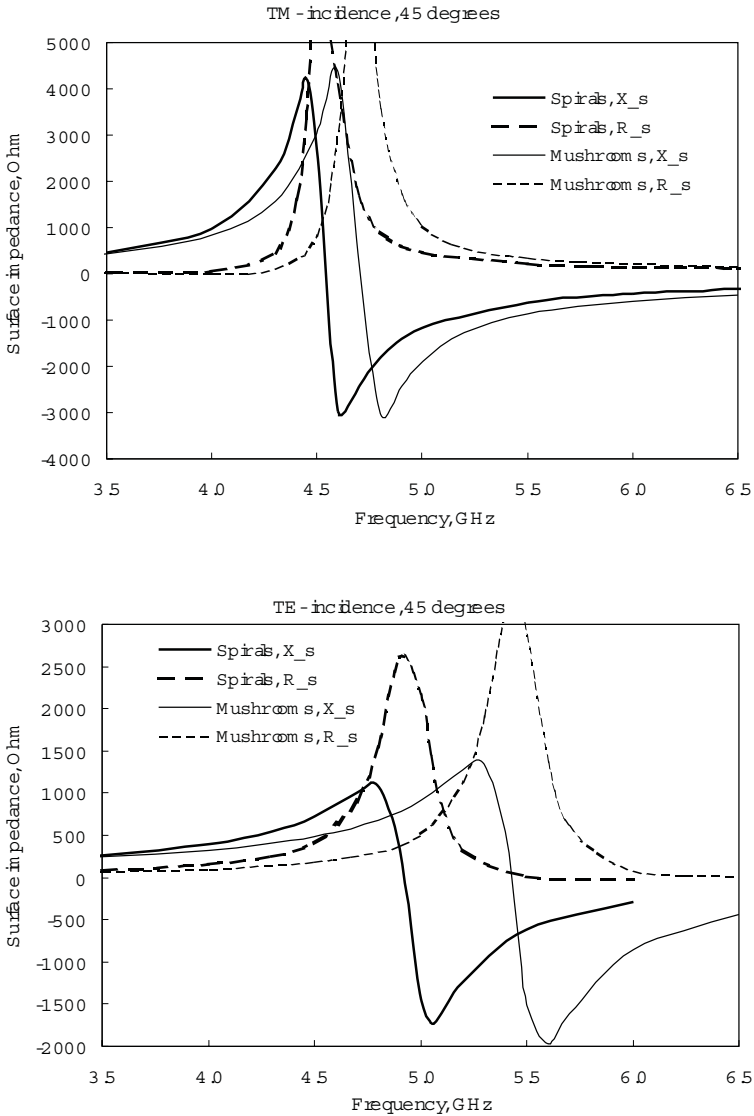
Figure 9. The surface impedance of two structures under comparison (HFSS simulations). TM- and TE-incidence. Thick lines: the structure containing a grid of spiral-shaped elements with loops. Thin lines: the mushroom structure.
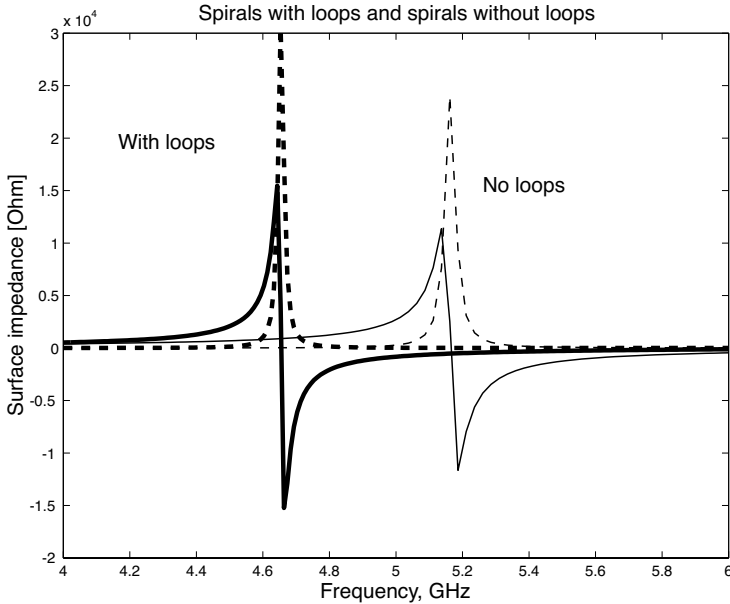
Figure 10. The surface impedance of two structures under comparison. Normal incidence. Thick lines: the structure containing a grid of spiral-shaped elements with loops. Thin lines: the structure containing a grid of spiral-shaped particles without loops.

So, our new structure is also more stable with respect to the incidence angle than two other structures for the TE-incidence. Our simple analytical model does not allow to obtain and explain this result. We suggest that this stabilization is related with the non-symmetry of the spiral-shaped element, which is stressed by the presence of the loops. This non-symmetry can lead to arising of some induced charge at the center of the element excited by a horizontal external field. Then, a vertical component of the electric field appears at the point to which the via is connected, leading to its excitation. Therefore the vias play their stabilizing role even for the TE-case.

5. CONCLUSION

In this paper, three different artificial impedance surfaces, based on periodic arrays of planar metal strips on a dielectric slab backed by a metal surface, are considered. All the elements are connected to the ground metal plane (substrate) with via wires.

One of the HIS is the so called mushroom structure, which is well-known. The second structure consist of an array of spiral elements with a small central patch. This geometry was recently suggested in [6] in order to stabilize the surface impedance with respect to variations of the incident angle. Such stabilization has been confirmed in [6] for the TM-polarization of incident plane waves. In the case of the TE-polarization no such advantage was found for the array of spiral elements. Furthermore, the resonant frequency of an array of spirals elements [6] is higher than for the mushroom structure with the same period and the slab thickness which is a disadvantage of such spiral structures.

The third structure is suggested in the present paper. This structure is composed of spiral elements with four square loops but without a central patch. Thus, a further reduction of the area of the metal surface is reached while the other parameters of the structure are fixed. Comparison of the third variant with the first and the second ones performed in this paper has shown that the spiral structure suggested here allows us to reduce resonant frequency with respect to the first and second structures for the fixed grid period and substrate thickness. From the other side, this effect means that for a fixed resonant frequency the period of the structure or the thickness of the dielectric layer can be reduced, allowing to reduce the overall structure thickness and weight.

For obliquely incident waves of both TM and TE-polarizations we also obtain a reduction of the resonant frequency (in comparison with two other structures), and a better stabilization of the frequency dependence of Z_s with respect to variations of the incident wave angle. For example, for $\theta = 0 \ldots \pi/4$ we have obtained the resonant frequency shift of -2.8 percent for TM-polarization and $+4.9$ percent for TE-polarization. For the mushroom structure the corresponding resonant frequency shifts are -4.5 and $+10.4$ percent, respectively. For the structure with spiral elements without loops this frequency shift makes $+1$ and $+7$ percent, respectively. Thus, we can conclude that the structure we suggest in the present work is prospective for antenna applications.

REFERENCES

1. Poilasne, G., J. Lenormand, P. Pouliguen, K. Mahdjoubi, C. Terret, and P. Gelin, "Theoretical study of interactions between antennas and metallic photonic band-gap structures," *Microw. Opt. Technol. Lett.*, Vol. 31, 214–219, 2001.

2. Sievenpiper, D., R. F. Zhang, F. J. Broas, N. G. Alexopoulos,

and E. Yablonovich, "High-impedance electromagnetic surfaces with a forbidden frequency band," *IEEE Trans. Microw. Theory Techniques*, Vol. 47, 2059–2074, 1999.

3. Yang, F.-R., K. P. Ma, Y. Qian, and T. Itoh, "A novel TEM waveguide using uniplanar compact photonic band-gap (UC-PBG) structure," *IEEE Trans. Microw. Theory Techniques*, Vol. 47, 2092–2098, 1999.

4. Sievenpiper, D., "High-impedance electromagnetic surfaces," Ph.D. Dissertation, UCLA, 1999. Available at www.ee.ucla.edu/labs/photon/thesis/ThesisDan.pdf.

5. Tretyakov, S. A. and C. R. Simovski, "Dynamic model of artificial impedance surfaces," *J. Electromagn. W. Applic.*, Vol. 17, 131–145, 2003.

6. Simovski, C. R., S. A. Tretyakov, and P. de Maagt, "Artificial high-impedance surfaces: analytical theory for oblique incidence," *Antennas and Propagation Society International Symposium*, Vol. 1, 2003.

7. Belov, P. A., R. Marques, M. G. Silveirinha, I. S. Nefedov, C. R. Simovski, and S. A. Tretyakov, "Strong spatial dispersion in wire media in the very long wavelength limit," *Physical Review B*, Vol. 76, 113103 (1–5), 2003.

8. Lindell, I. H., *Methods of Electromagnetic Fields Analysis*, London, Clarendon Press, 1992.

9. Andersson, I., "On the theory of self-resonant grids", *The Bell System Technical Journal,* Vol. 55, 1725–1731, 1975.

10. Sievenpiper, D. F. and E. Yablonovich, "3D metallp-dielectric photonic crystals with strong capacitive coupling between metallic islands," *Phys. Rev. Lett.*, Vol. 80, 2829–2832, 1998.

11. Kalantarov, P. L. and L.A. Tseitlin, *Calculation of inductances*, Moscow, Radio i Sviaz, 1986 (in Russian).